Electronic Supplementary Material (ESI) for Journal of Materials Chemistry A.

Electronic Supplementary Information for:

Enhanced electrocatalytic performance of Pt nanoparticles on triazine-functionalized graphene nanoplatelets for both oxygen and iodine reduction reactions

In-Yup Jeon,[1,2,†] Do Hyung Kweon,[1,†] Seong-Wook Kim,[1] Sun-Hee Shin,[1] Yoon Kwang Im,[1] Soo-Young Yu,[1] Myung Jong Ju[1,*] and Jong-Beom Baek[1,*]

[1] School of Energy and Chemical Engineering/Center for Dimension-Controllable Covalent Organic Frameworks, Ulsan National Institute of Science and Technology (UNIST), UNIST-gil 50, Ulsan, 44919, Korea

[2]Department of Chemical Engineering, Wonkwang University, Iksandae-ro 460, Iksan, Jeonbuk 54538, Republic of Korea

E-mails: jmj12@unist.ac.kr, jbbaek@unist.ac.kr

[†] These authors contributed equally to this work.

Experimental Section

Instrumentations. Fourier transform infrared (FT-IR) spectra were recorded on Perkin-Elmer Spectrum 100 using KBr disks. Elemental analysis (EA) was conducted with Thermo Scientific Flash 2000. The field emission scanning electron microscopy (FE-SEM) was performed on FEI Nanonova 230. The high-resolution transmission electron microscopy (HR-TEM) was performed on JEOL JEM-2100F microscope. The TEM specimen were prepared by dipping carbon micro-grids (Ted Pella Inc., 200 Mesh Copper Grid) into well-dispersed samples in ethanol. Themogravimetric analysis (TGA) was conducted on a TA Q200 (TA Instrument) at a heating rate of 10 °C min^{-1} under air. The surface area was measured by nitrogen adsorption-desorption isotherms using the Brunauer-Emmett-Teller (BET) method on Micromeritics ASAP 2504N. X-ray photoelectron spectra (XPS) were recorded on a Thermo Fisher K-alpha XPS spectrometer. X-Ray diffraction (XRD) patterns were recorded with a Rigaku D/MAZX 2500V/PC with Cu-Kα radiation (35 kV, 20 mA, $\lambda = 1.5418$ Å).

Electrochemical Measurements. The electrochemical measurements were conducted using a computer-controlled potentiostat (1470E Cell Test System, Solartron Analytical, UK) with a typical three-electrode cell. A platinum wire was used as a counter-electrode and Ag/AgCl (Saturated KCl) electrode as the reference electrode. All the experiments were conducted at ambient condition. The working electrodes were prepared by applying respective catalyst inks onto the pre-polished glassy carbon (GC) disk electrodes. Briefly, samples were dispersed in H_2O and ultrasonicated for 5 min to form uniform catalyst inks (2 mg mL^{-1}). A total of 10 μL of a well-dispersed catalyst ink was applied onto a pre-polished GC disk electrode (5 mm in diameter). After drying at room temperature, Nafion (0.05 wt%) stock solution (1 μL) in ethanol was applied onto the surface of the catalyst layer to form a thin protective film. The addition of a small amount of Nafion could effectively improve the dispersion of catalyst suspension. The electrodes thus prepared were dried at room temperature overnight prior to the electrochemical tests. The detailed kinetic analysis was conducted according to Koutecky-Levich plots:

$$\frac{1}{j}=\frac{1}{j_k}+\frac{1}{B\omega^{0.5}} \tag{S1}$$

where j_k is the kinetic current and B is Levich slope which is given by:

$$B = 0.2nF(D_{O_2})^{2/3}\upsilon^{-1/6}C_{O_2} \tag{S2}$$

Here n is the number of electrons transferred in the reduction of one O_2 molecule, F is the Faraday constant (F = 96490 C/mol), D_{O2} is the diffusion coefficient of O_2 ($D_{O2} = 1.67\times10^{-5}$ cm^2 s^{-1}), C_{O2} is concentration of O_2 in the solution ($C_{O2} = 1.38 \times 10^{-6}$ mol cm^{-3}), and ν is the kinematics viscosity for 0.1 M $HClO_4$ (v = 0.01 cm^2 s^{-1}).[S1] The constant 0.2 is adopted when the rotation speed is expressed in rpm. According to equations (1) and (2), the number of electrons transferred (n) can be obtained from the slope of Koutecky-Levich plot of i^{-1} *vs.* $\omega^{-1/2}$.[S2,S3]

Fabrication and Measurement of Single PEM Fuel Cell. The catalyst inks were prepared by mixing the catalysts with Nafion (5 wt%, CNL energy). The commercial Pt/C catalysts (40 wt%) was dispersed by isopropanol at ionomer/catalyst ratio (3/10). Pt/TfGnP was dispersed by isopropanol at ionomer/catalyst ratio (1/10). The catalyst inks were sonicated for 30 minutes and then sprayed onto a 1.44 cm^2 gas diffusion layer (GDL, Toray TGP-H-060) using electrospray. The anode was the commercial Pt/C catalysts with 0.4 mg cm^{-2} to ensure sufficient proton supply from the anode. The commercial Pt/C catalysts as cathode had 0.4 mg cm^{-2} and Pt/TfGnP as cathode had 0.7 mg cm^{-2}. A pair of cathode and anode was hot pressed onto either sides of a NRE-212 (Nafion®, Alfa Aesar) membrane at 130 °C for 60s under no pressure and 10s under pressure 2.5 MPa. The membrane electrode assembly (MEA) was tested with 1 cm^2 gasket at 75 °C. Pure H_2 (200 mL min^{-1}) and O_2 (600 mL min^{-1}) were used as anode and cathode fuels.

Preparation of Electrodes for IRR. Homogeneously dispersed 0.1 wt% sample powders in 2-propanol solution were obtained by ultrasonication for 30 min. The resultant solution was deposited directly onto on fluorine-doped SnO_2 (FTO)/glass (TEC-8, Pilkington) using an e-spray method. First, the sample dispersion solutions were loaded into a plastic syringe equipped with a 30-gauge stainless steel hypodermic needle. The needle was connected to a high voltage power supply (ESN-HV30). A voltage of ~ 4.3 kV was applied between a metal orifice and the conducting substrate at a distance of 8 cm. The feed rate was controlled by the syringe pump (KD Scientific Model 220) at a constant flow rate of 70 μL min^{-1}. The electric field overcomes the surface tension of the droplets, resulting in the minimization of numerous charged mists. The resultant electrodes were sintered at 300 °C for 30 min at atmosphere prior to device fabrication. For the reference, the Pt-FTO electrode was also prepared by deposition of *ca.* 30 μL cm^{-1} of H_2PtCl_6 solution (2 mg of H_2PtCl_6 in 1 mL of ethanol) and sintered at 400 °C for 15 min. SEM images of the TfGnP and Pt/TfGnP deposited FTO (Fig. S12) exhibited similar surface morphologies.

Fabrication of Symmetrical Dummy Cells. Symmetrical sandwich-typed dummy cells were fabricated with two identical Pt-, TfGnP- or Pt/TfGnP-FTO sheets, which were separated by 25-μm thick Surlyn (Solaronix, Switzerland) tape as a sealant and spacer leaving a 0.6 × 0.6 cm^2 active area. The sheet edges were coated by an ultrasonic soldering system (USS-9200, MBR Electronics) to improve electrical contacts. Electrolyte solution was composed of 0.6 M 1,2-dimethyl-3-propylimidazolium iodide (DMPII), 0.1 M LiI, 0.05 M I_2, and 0.5 M TBP in acetonitrile. Electrolyte solution was introduced through a drilled hole on the CE *via* vacuum backfilling. The hole was sealed with cover glass using a Surlyn seal.

Fabrication and Characterization of DSSCs. FTO plates were cleaned in detergent solution, water, and ethanol using an ultrasonic bath. The FTO substrates were immersed in 40 mM aqueous $TiCl_4$ solution at 70 °C for 30 min and washed with water and ethanol. A TiO_2 colloidal paste (18NR-T, Dyesol) was screen-printed onto FTO/glass and sintered at 500 °C for 30 min in air. The thickness of the transparent layer was measured using an Alpha-step 250 surface profilometer (Tencor Instruments), and a paste for the scattering layer containing 500-nm-sized anatase particles (STP-500N, ENB Korea) was screen printed and then dried for 2 hours at 25 °C. The TiO_2 electrodes were sintered at 500 °C for 30 min. The resulting TiO_2 photoanodes were immersed in a THF/ethanol (v/v, 2:1) solution 0.3 mM N719 sensitizer and kept at room temperature for 12 hours. The dye-adsorbed TiO_2 photoanodes were assembled with Pt-, TfGnP-, or Pt/TfGnP-CEs using a thermal adhesive film (25-mm-thick Surlyn, DuPont) as a spacer to produce a sandwich-type cell. Electrolyte solution was introduced through a drilled hole on the CEs via vacuum backfilling. The hole was sealed with cover glass using Surlyn. The light intensity was adjusted with a Si solar cell that was doubled-checked with a National Renewable Energy Laboratory-calibrated Si solar cell (PV Measurement Inc.). The applied potential and cell current were measured using a Keithley digital source meter (model 2400). Photoelectrochemical data were measured using a 1000-W xenon light source (Oriel, 91193) that was focused to give 100 mW cm^{-2} (1 sun at AM 1.5 G). The J-V characteristics of the cell under these conditions were determined by externally biasing the cell and measuring the generated photocurrent. This process was fully automated using the Wave-Metrics software.

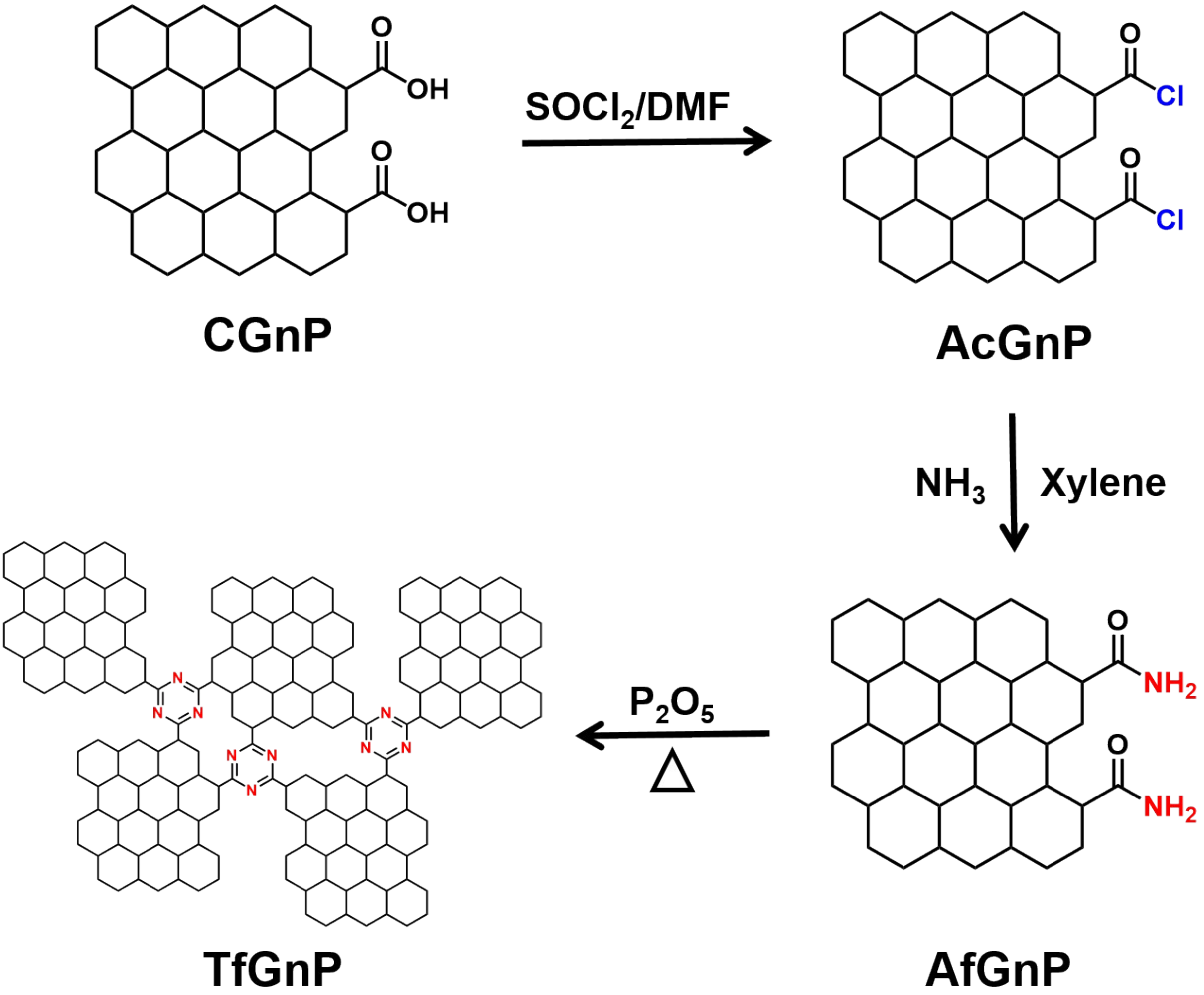

Scheme S1 Schematic representation for the preparation of triazine-functionalized graphene nanoplatelets (TfGnP) as Pt supporter driven from carboxylic acid-functionalized graphene nanoplatelets (CGnP).

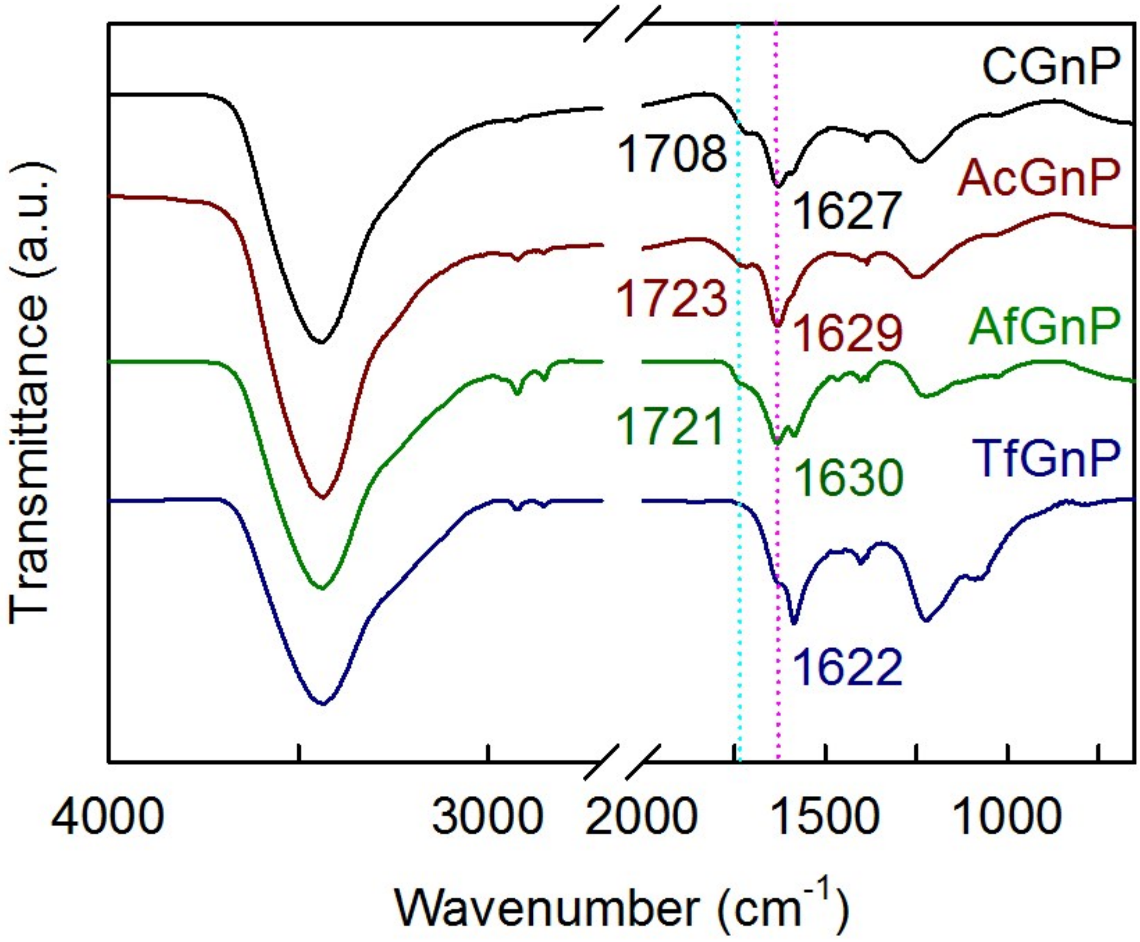

Fig. S1 FT-IR spectra (KBr pellets) of CGnPs, AcGnP, AfGnP and TfGnP.

FT-IR spectroscopy was used as convenient and informative analytical tool to monitor the change of functional groups. Through the comparing each sky blue and red line peak, we could confirm exactly and easily the alteration of the functional groups of GnP. CGnP, AcGnP and AfGnP showed the adsorption bands corresponding to the enol (1708, 1723 and 1721 cm^{-1}, sky blue line) and keto (1627, 1629 and 1630 cm^{-1}, red line) tautomer's, respectively. However, TfGnP showed only C=N bond peak of triazine at 1,622 cm^{-1} but disappeared C=O bond peak. We deduced that the carboxylic acid groups (-COOH) at the edge of GnP was changed into acyl chloride (-COCl), amide (-CONH$_2$) and triazine, in that order.

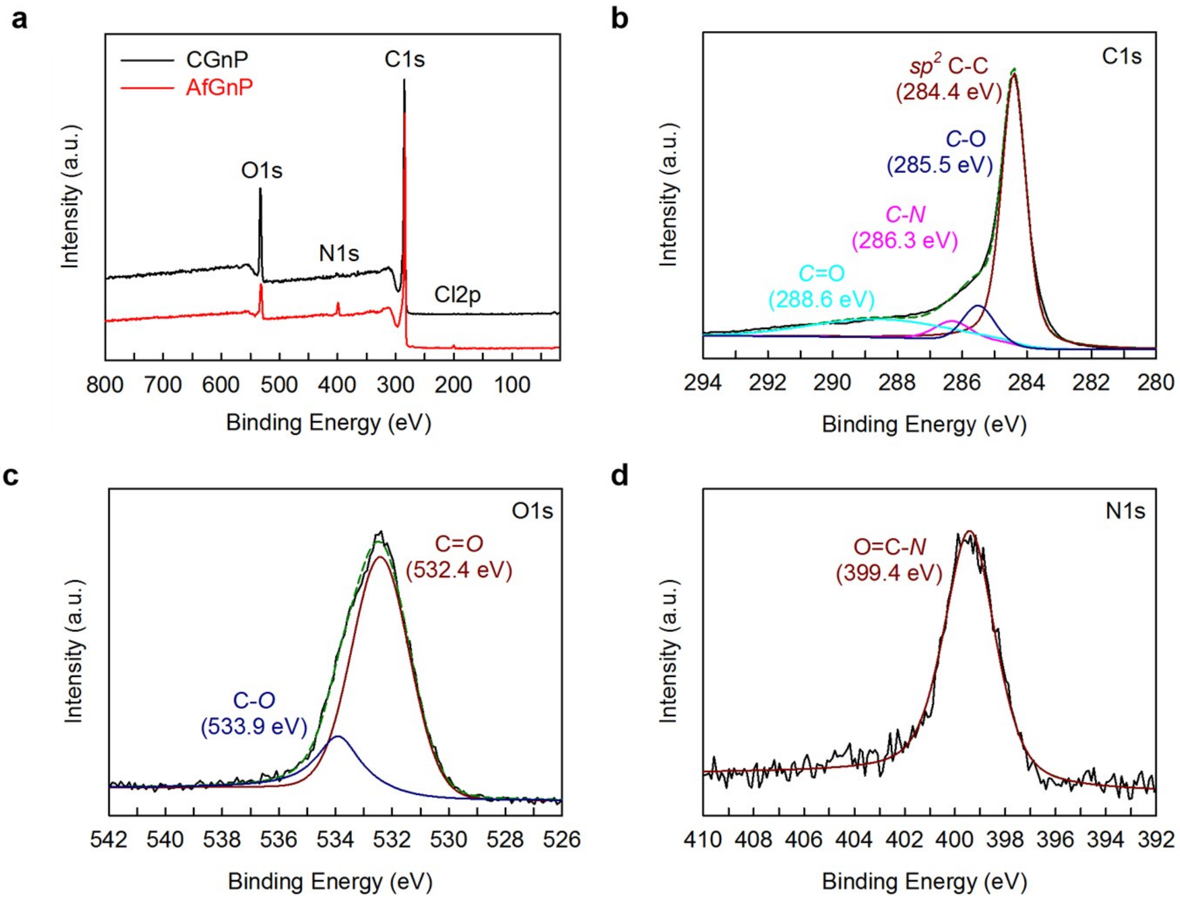

Fig. S2 (a) XPS full-scale survey spectra of CGnP and AfGnP. High-resolution XPS survey spectra of AfGnP: (b) C1s; (c) O1s; (d) N1s.

The survey spectrum of CGnP showed a main C1s peak and O1s peak which is mostly related to carboxylic acid[S4] while AfGnPs showed N1s characteristic peak along with C1s, O1s and Cl2p which is adsorbed physically on the surface of AfGnP (Fig. S2). And also, the content of N contained AfGnP is about 2.67 at% (Table S2). High-resolution XPS spectra together with the curve fittings and deconvolutions, showed that the C1s peak of AfGnP consisted of *sp*^{2} C-C (284.4 eV), *C*-O (285.5 eV), *C*-N (286.3 eV) and *C*=O (288.6 eV) (Fig. S2b) and O1s peak of consisted of C=*O* (532.4 eV) and C-*O* (533.9 eV) (Fig. S2c). The N1s spectrum were comprised of O=C-N (399.4 eV) peak (Fig. S2d)[S5,S6], indicating that carboxylic acid groups of CGnP converted into amide groups as schematically represented in Scheme S1.

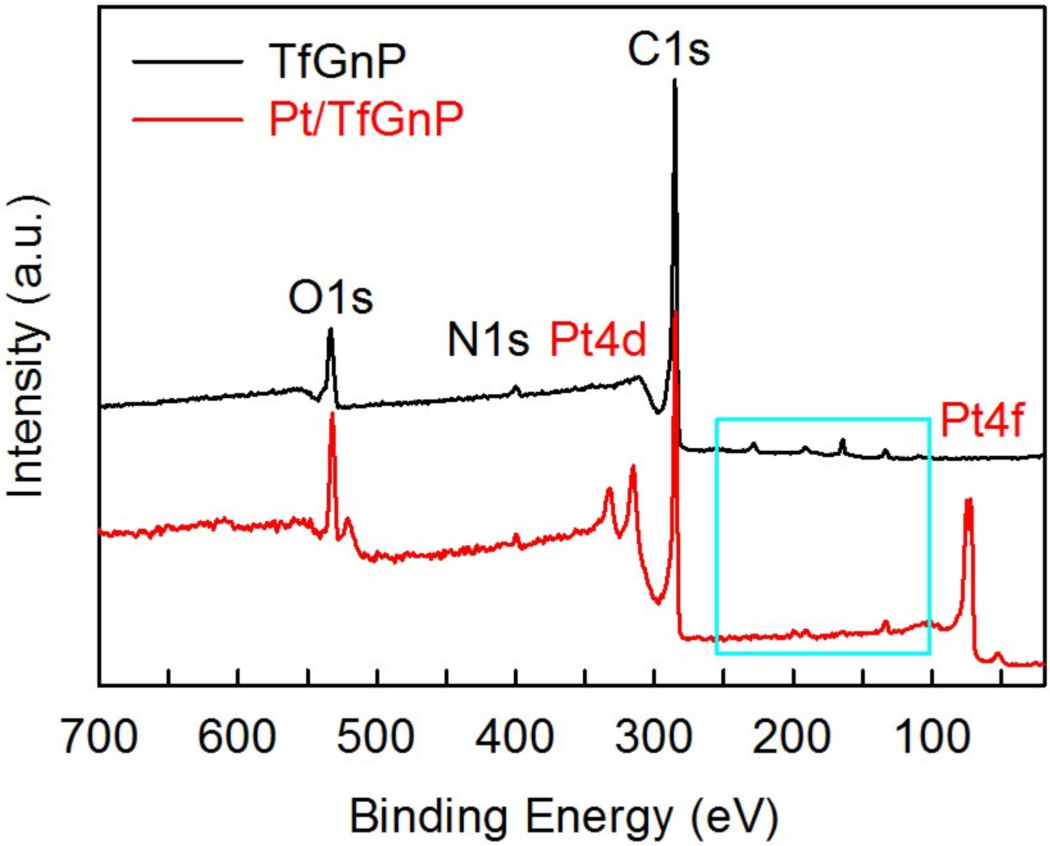

Fig. S3 XPS full-scale survey spectra of TfGnP and Pt/TfGnP.

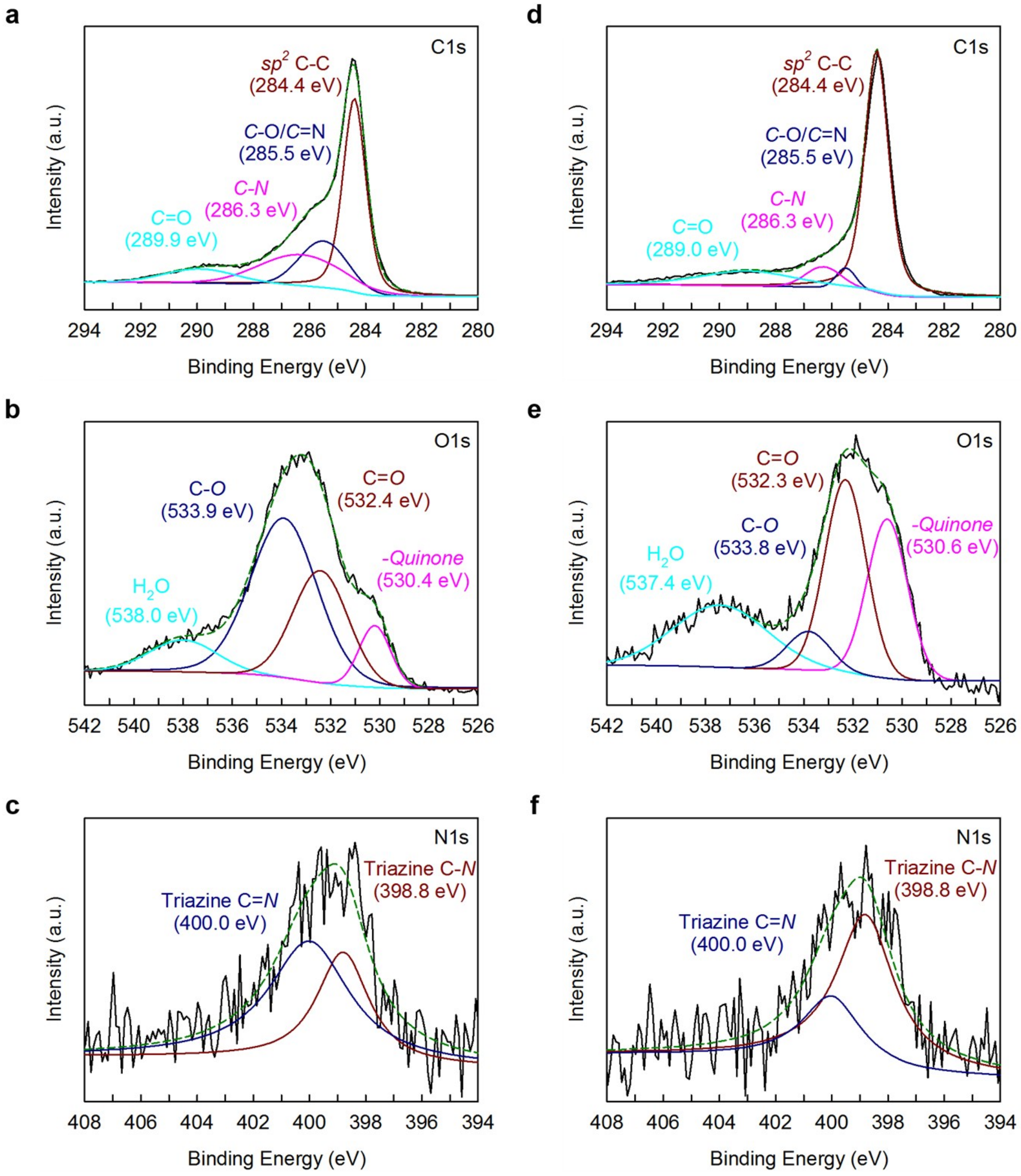

Fig. S4 High-resolution XPS survey spectra of (a, b and c) TfGnP and (d, e and f) Pt/TfGnP: (a, d) C1s; (b, e) O1s; (c, f) N1s.

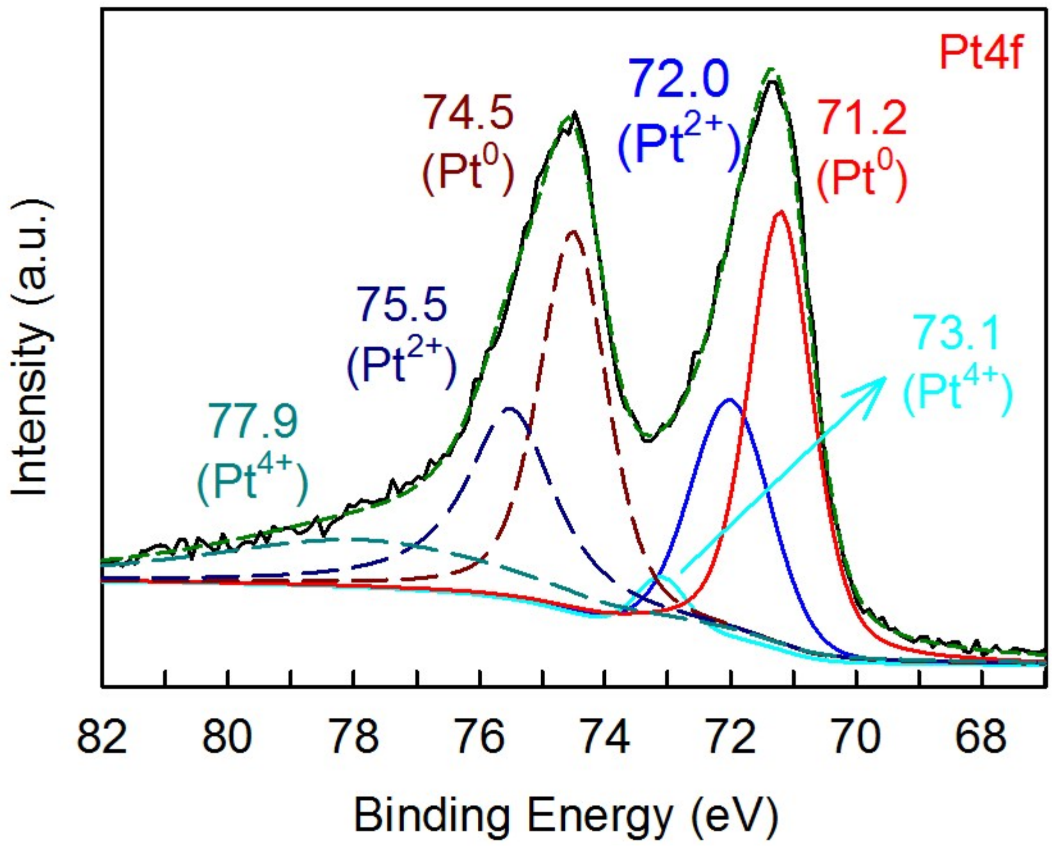

Fig. S5 High-resolution XPS survey spectra of Pt4f for Pt/TfGnP.

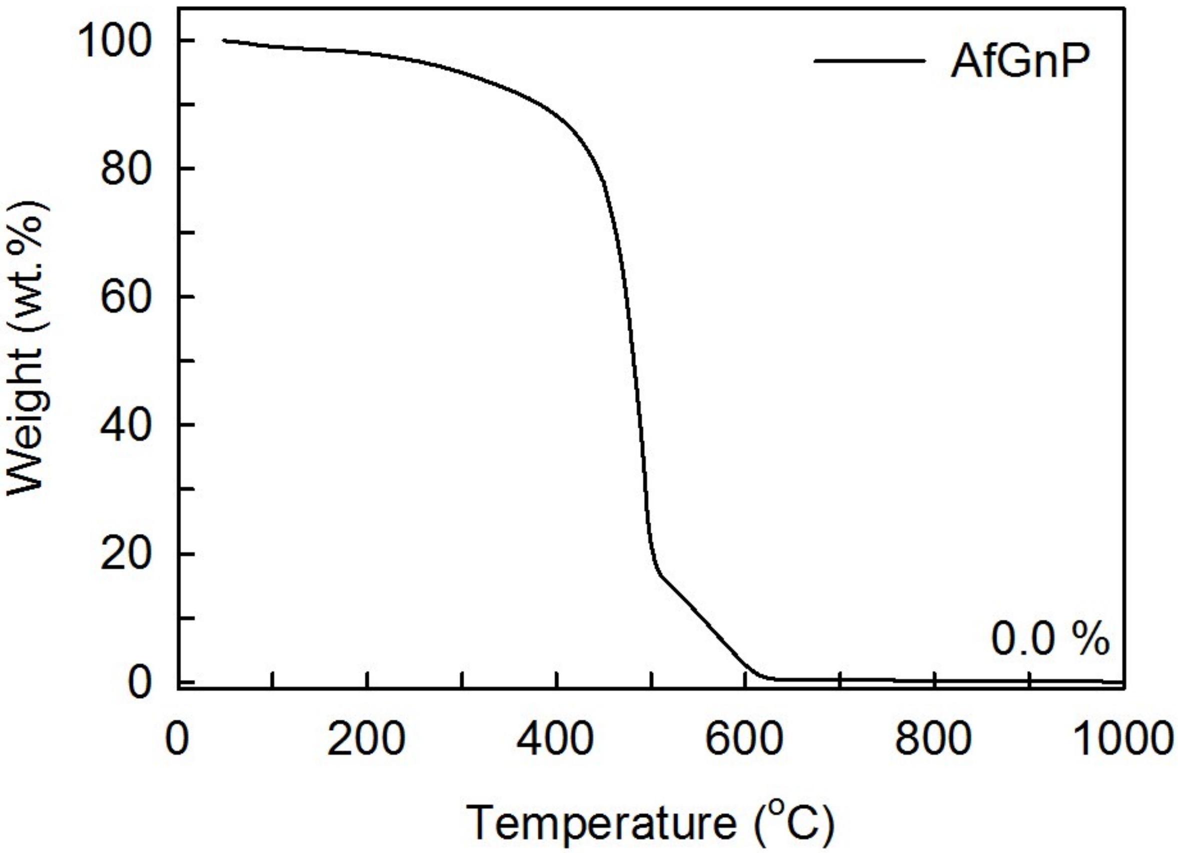

Fig. S6 TGA thermograms of AfGnP obtained in air at the heating rate of 10 °C min^{-1}.

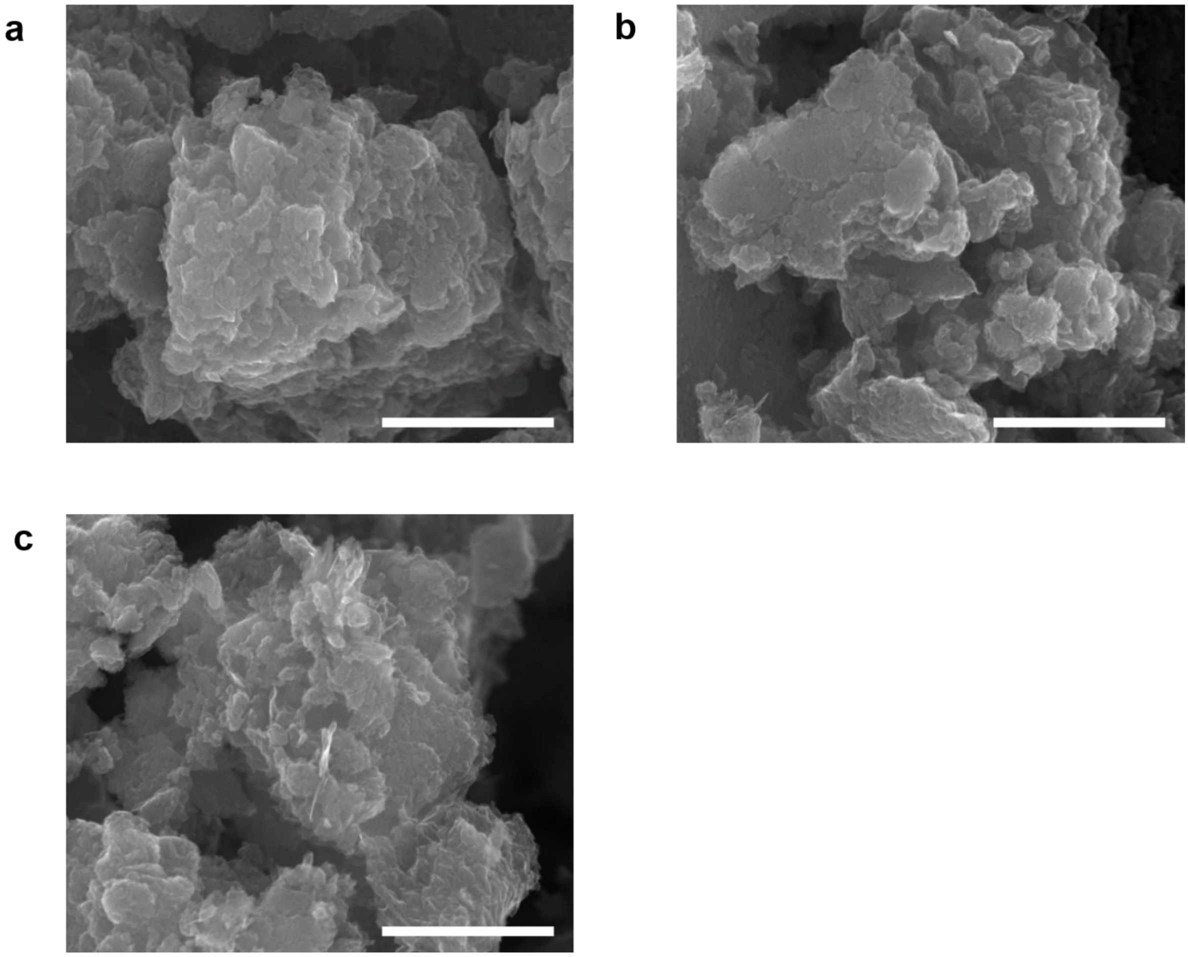

Fig. S7 FE-SEM images: (a) CGnP; (b) AfGnP; (c) TfGnP. Scale bars are 1 μm.

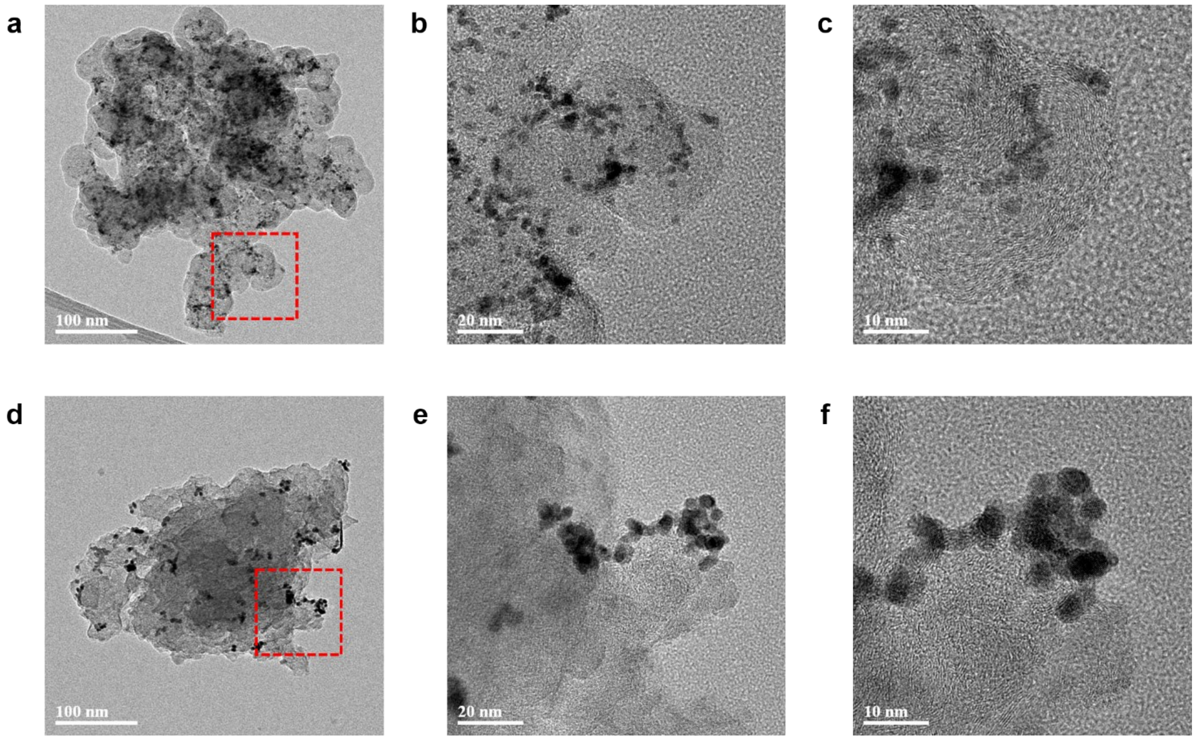

Fig. S8 HR-TEM images: (a, b, c) the commercial Pt/C catalysts; (d, e, f) Pt/TfGnP.

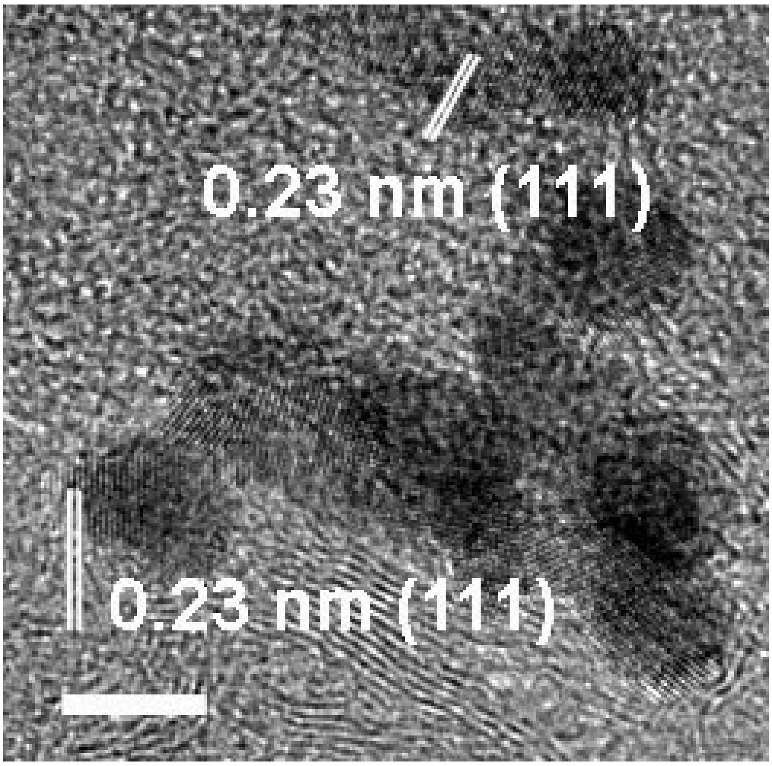

Fig. S9 Highly magnified TEM image and crystal lattice fringe of Pt/TfGnP. Scale bar is 5 nm.

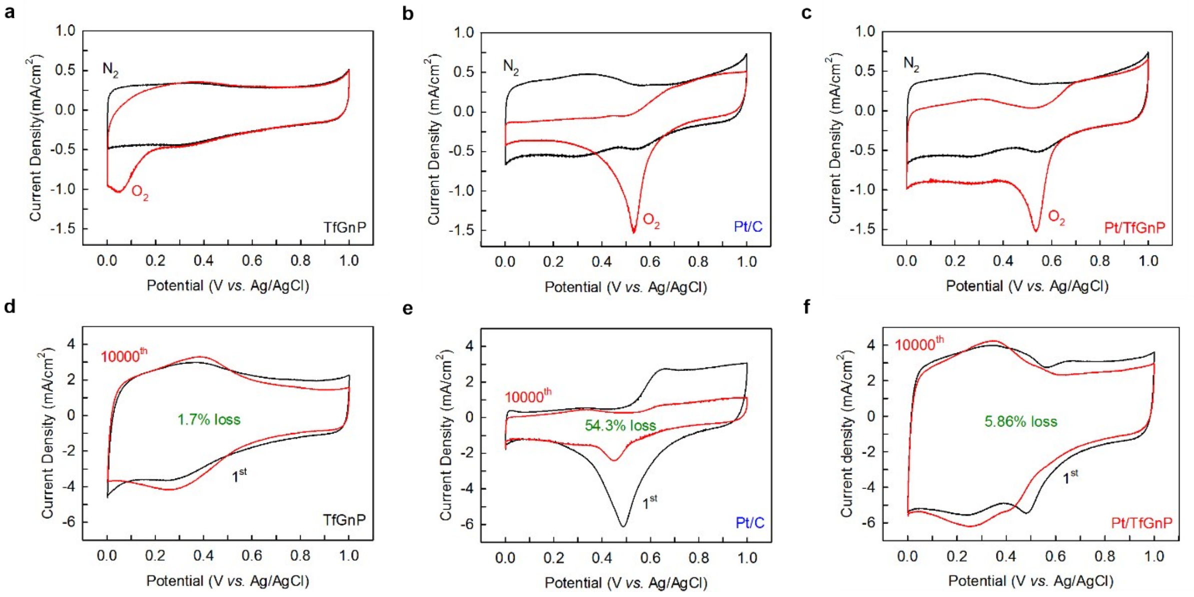

Fig. S10 Cyclic voltammograms (CV) of samples in N_2- and O_2-saturated 0.1 M aq. $HClO_4$ solution with a scan rate of 10 mV s^{-1}: (a) TfGnP; (b) The commercial Pt/C catalysts; (c) Pt/TfGnP. CV curves of samples 1st and 10,000th cycles with scan rate of 100 mV s^{-1} in O_2-saturated 0.1 M aq. $HClO_4$ solution: (d) TfGnP; (e) The commercial Pt/C catalysts; (f) Pt/TfGnP.

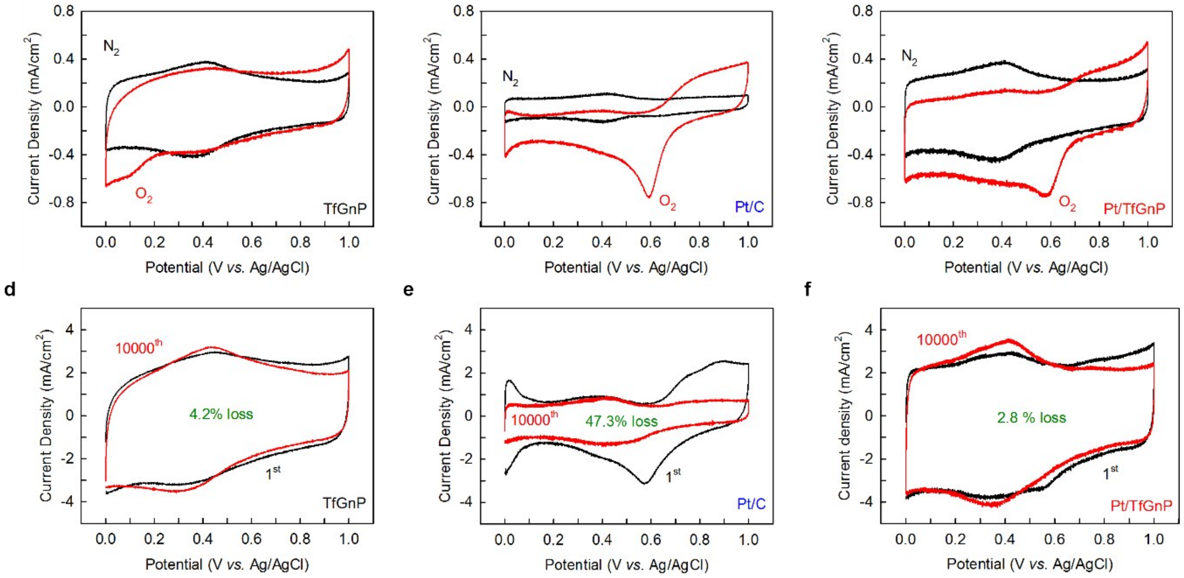

Fig. S11 Cyclic voltammograms (CV) of samples in N_2- and O_2-saturated 0.5 M aq. H_2SO_4 solution with a scan rate of 10 mV s^{-1}: (a) TfGnP; (b) The commercial Pt/C catalysts; (c) Pt/TfGnP. CV curves of samples 1st and 10,000th cycles with scan rate of 100 mV s^{-1} in O_2-saturated 0.5 M aq. H_2SO_4 solution: (d) TfGnP; (e) The commercial Pt/C catalysts; (f) Pt/TfGnP.

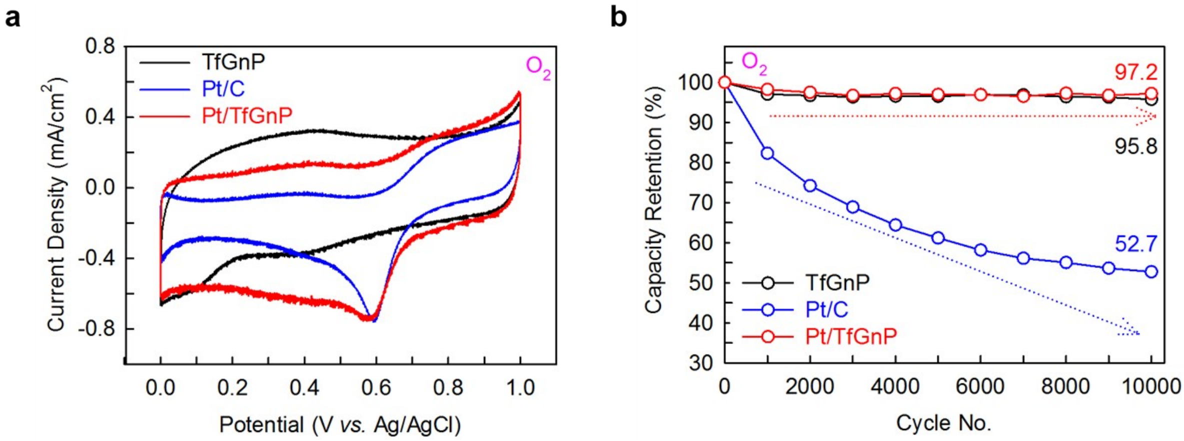

Fig. S12 (a) Cyclic voltammograms (CV) in O_2-saturated 0.5 M aq. H_2SO_4 solution at a scan rate of 10 mV s^{-1} with TfGnP, the commercial Pt/C catalysts and Pt/TfGnP. (b) Capacity retention of TfGnP, the commercial Pt/C catalysts, Pt/TfGnP at a scan rate of 100 mV s^{-1}.

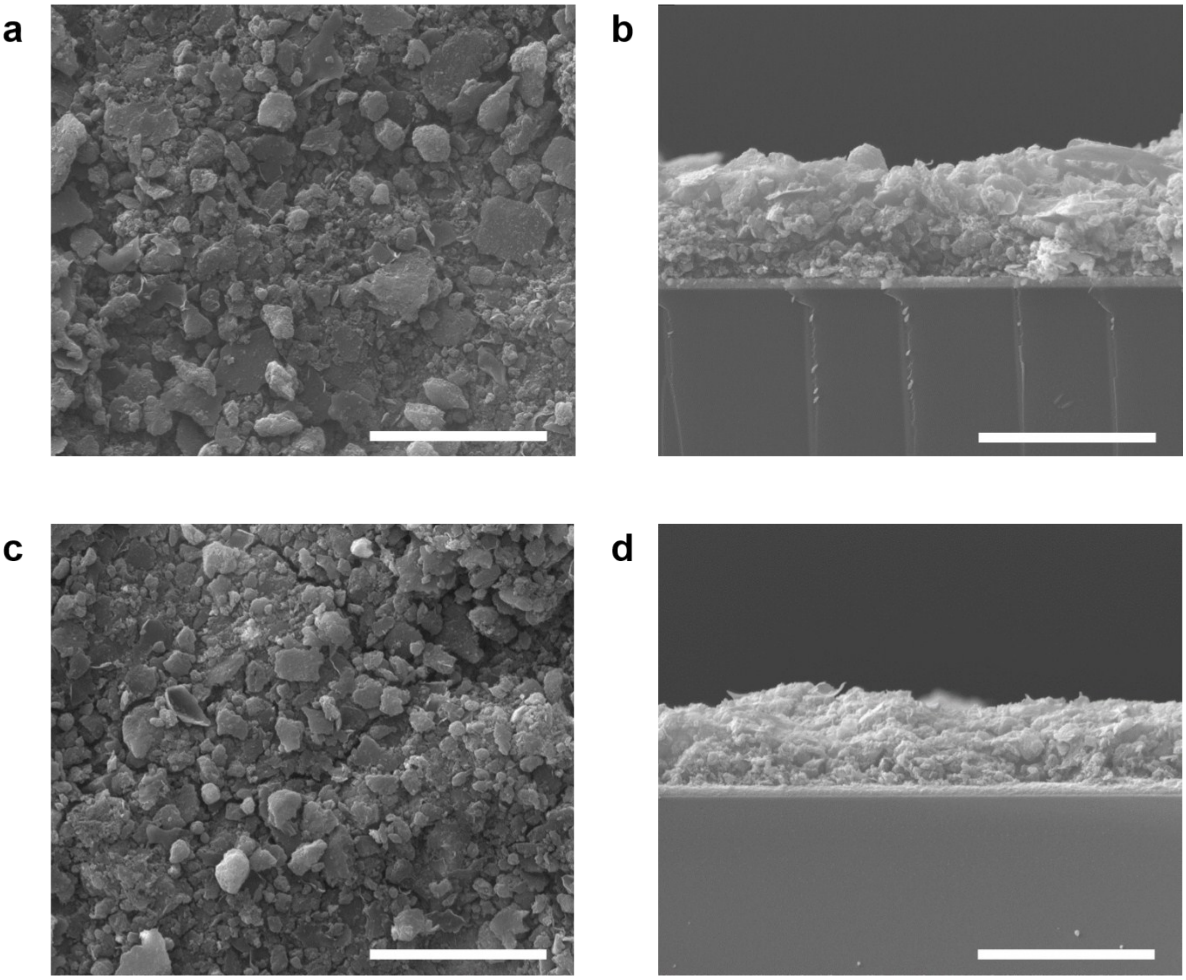

Fig. S13 SEM images of TfGnP and Pt/TfGnP on FTO substrate: Top view images of (a) TfGnP and (c) Pt/TfGnP; Cross section view images of (b) TfGnP and (d) Pt/TfGnP.

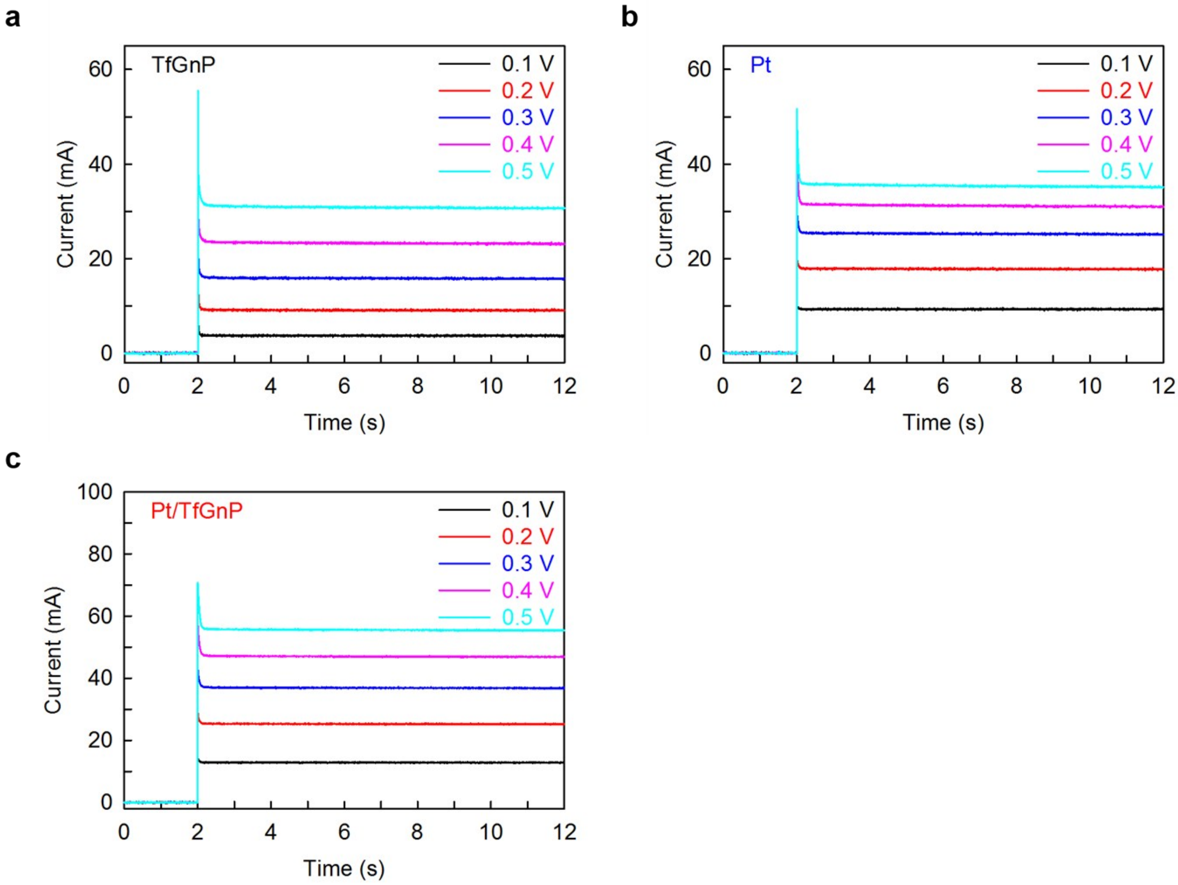

Fig. S14 Potential-step chronoamperometry (CA) curves on symmetrical dummy cells. Potential was from 0.1 to 0.5 V for 10 s: (a) Pt; (b) TfGnP; (c) Pt/TfGnP. The forward step, that is, the transition potential is initially from E_1 to E_2 for a short time, and then is applied in a series of potentials. For a period *t*, it causes a buildup of the current due to the oxidation product in the region near the electrode.

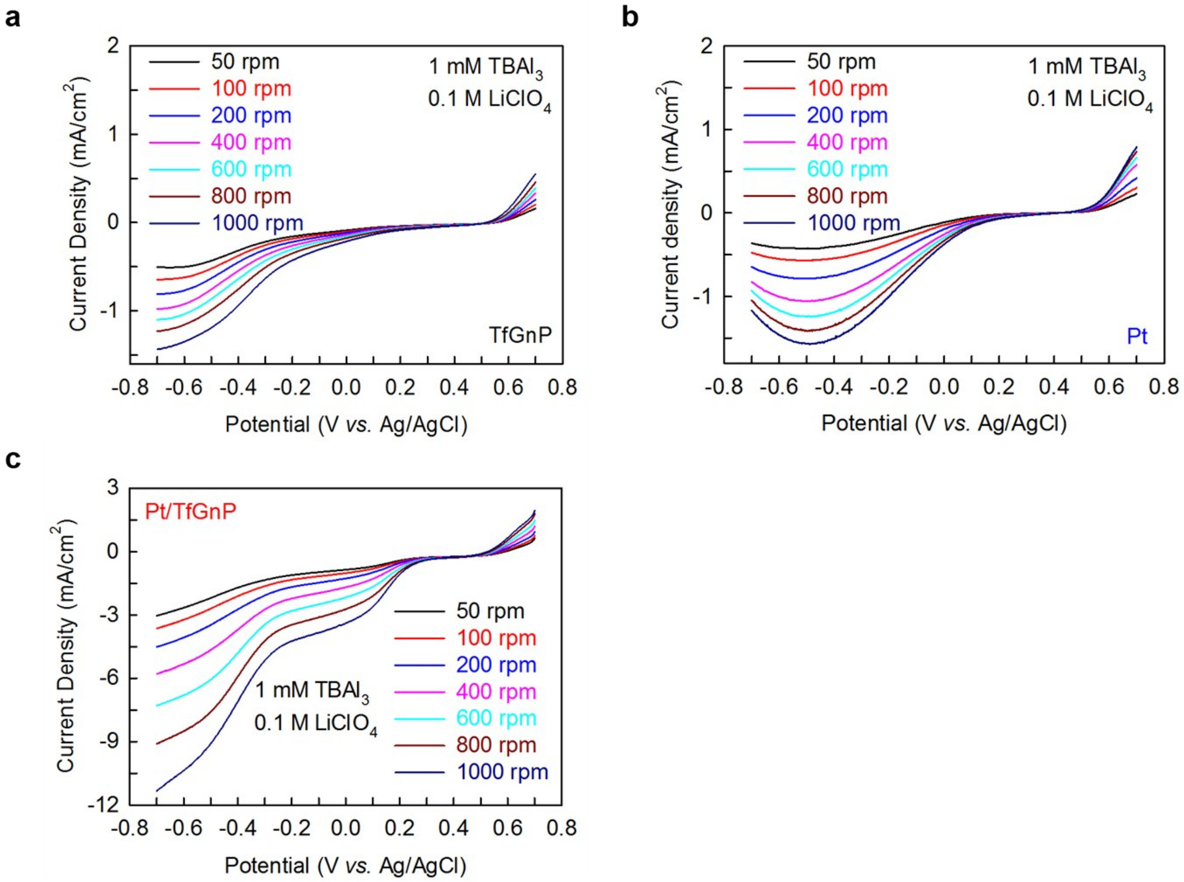

Fig. S15 RDE curves on the IRR by using TfGnP, Pt and Pt/TfGnP electrodes with different scan rate. Glassy carbon electrodes coated with TfGnP and Pt/TfGnP films, and a Pt disk electrode were used as the working electrode. A Pt wire and an Ag/AgCl were used as the counter and reference electrodes, respectively. The potential scan rate for RDE analysis was set at 2 mV s^{-1}. The electrolyte was composed of 1.0 mM tetrabutyl ammonium triiodide (TBAI$_3$) and 0.1 M LiClO$_4$ in acetonitrile.

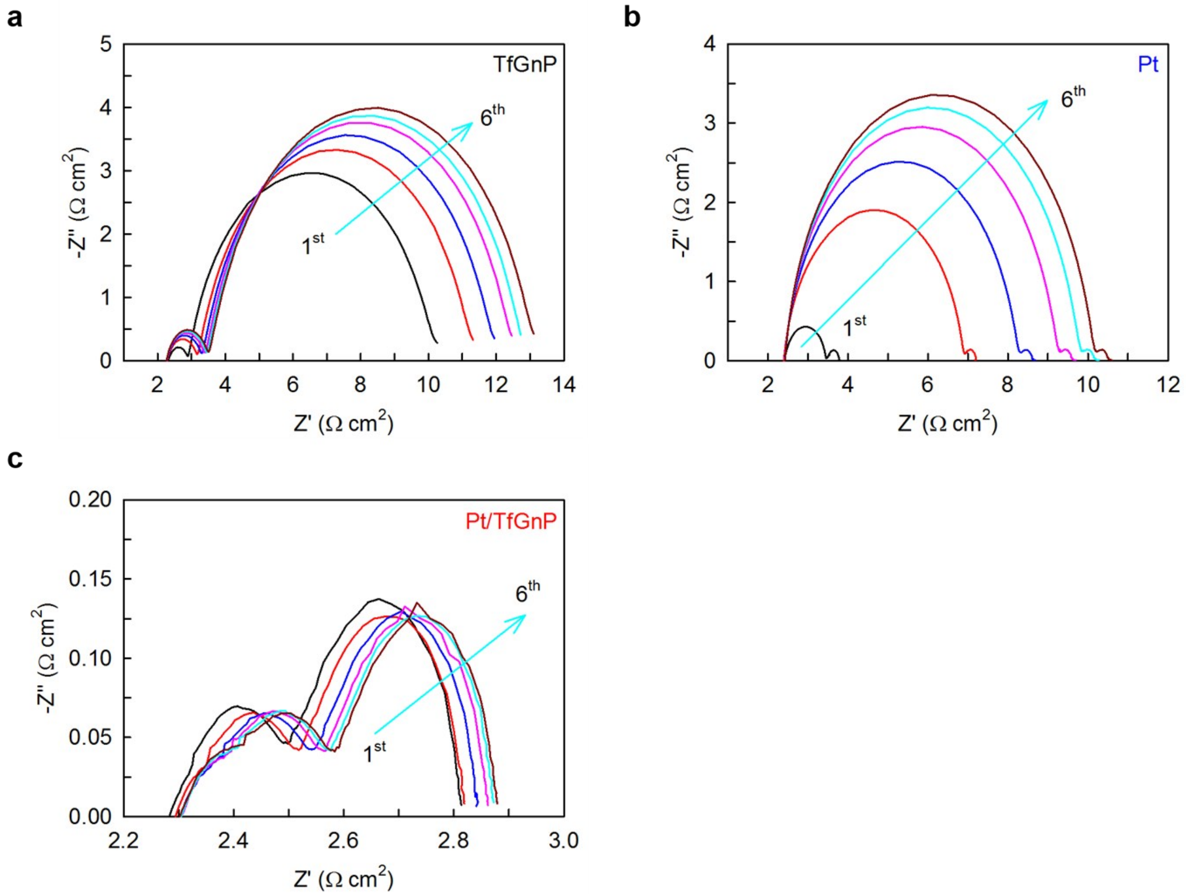

Fig. S16 Nyquist plots of the symmetrical dummy cells with different electrodes. The sequence of measurements is as follows: 200 × CV scans (from 0 V → 1 V → −1 V → 0 V at a scan rate of 50 mV s^{-1}) followed by 60 s relaxation at 0 V and then EIS measurement at zero bias potential. The sequence of electrochemical test was repeated 5 times. (a) TfGnP; (b) Pt; (c) Pt/TfGnPs.

Table S1. Elemental analysis (EA) data of CGnP, AfGnP and TfGnP

	C (wt%)	H (wt%)	O (wt%)	N (wt%)
CGnP	73.26	1.59	24.84	-
AfGnP	76.65	1.26	13.91	4.96
TfGnP	78.74	1.74	15.66	2.43

Table S2. BET surface area, pore volume and pore size of CGnP, AfGnP and TfGnP

Sample	Surface Area ($m^2\ g^{-1}$)	Pore Volume ($mL\ g^{-1}$)	Pore Size (nm)
CGnP	635.8	0.601	3.78
AfGnP	634.0	0.591	3.73
TfGnP	963.0	0.760	3.15

Table S3. XPS data of CGnP, AfGnP, TfGnP and Pt/TfGnP

	C (at%)	O (at%)	N (at%)	Pt (at%)	Other (at%)
CGnP	85.51	14.49	-	-	-
AfGnP	88.72	7.91	2.67	-	0.71 (Cl)
TfGnP	83.59	10.37	2.00	-	2.22 (S)/1.91 (P)
Pt/TfGnP	78.53	9.64	2.71	2.32	2.90 (S)/2.78 (P) /1.11 (Cl)

Table S4. A catalytic performance of Pt/TfGnP and other Pt-based catalysts

Sample	Cycle retention	Cycle number	Electrolyte	Reference
Pt/TfGnP	94.2%	10000	0.1 M aq. $HClO_4$	This study
	97.2%	10000	0.5 M aq. H_2SO_4	
Pt/RGO/CB-1	>95%	20000	0.1 M aq. $HClO_4$	S7
Pt/RGO/CB-2	87%	20000	0.1 M aq. $HClO_4$	S7
Pt_n/gDNA-GO	94.2%	10000	0.1 M aq. $HClO_4$	S8
Pt nanoparticles/GO	67%	10000	0.1 M aq. $HClO_4$	S8
Pt/rGO	41%	10000	0.1M aq. $HClO_4$	S9
PtDs/gdsDNA/rGO	>90%	10000	0.1M aq. $HClO_4$	S9
PtNW/SG	58%	3000	0.1M aq. $HClO_4$	S10
PtNW/G	28%	3000	0.1M aq. $HClO_4$	S10
PFSA-Pt/G	>50%	2000	0.1M aq. $HClO_4$	S11
PtNW/SG	75%	1000	0.1M aq. $HClO_4$	S12
PtNT	80%	1000	0.5 M aq. H_2SO_4	S13
Pt/SWNT	84%	2160	0.1M aq. $HClO_4$	S14

References

S1 F. Fouda-Onana, S. Bah and O. Savadogo, *J. Electroanal. Chem.*, 2009, **636**, 1-9.

S2 C. Coutanceau, P. Crouigneau, J. Leger and C. Lamy, *J. Electroanal. Chem.*, 1994, **379**, 389-397.

S3 K. Hsueh, E. Gonzalez and S. Srinivasan, *Electrochim. Acta*, 1983, **28**, 691-697.

S4 I.-Y. Jeon, Y.-R. Shin, G.-J. Sohn, H.-J. Choi, S.-Y. Bae, J. Mahmood, S.-M. Jung, J.-M. Seo, M.-J. Kim and D. W. Chang, *Proc. Natl. Acad. Sci. U. S. A.,* 2012, **109**, 5588-5593.

S5 Y. An, M. Chen, Q. Xue and W. Liu, *J. Colloid Interface Sci.*, 2007, **311**, 507-513.

S6 D. Yu and L. Dai, *J. Phys. Chem. Lett.*, 2009, **1**, 467-470.

S7 Y. Li, Y. Li, E. Zhu, T. McLouth, C.-Y. Chiu, X. Huang and Y. Huang, *J. Am. Chem. Soc.*, 2012, **134**, 12326-12329

S8 J. N. Tiwari, K. Nath, S. Kumar, R. N. Tiwari, K. C. Kemp, N. H. Le, D. H. Youn, J. S. Lee and K. S. Kim, *Nat. Commun.*, 2013, **4**, 2221.

S9 J. N. Tiwari, K. C. Kemp, K. Nath, R. N. Tiwari, H.-G. Nam and K. S. Kim, *Acs Nano*, 2013, **7**, 9223-9231.

S10 M. A. Hoque, F. M. Hassan, D. Higgins, J. Y. Choi, M. Pritzker, S. Knights, S. Ye and Z. Chen, *Adv. Mater.*, 2015, **27**, 1229-1234.

S11 K.-W. Nam, J. Song, K.-H. Oh, M.-J. Choo, H. A. Park, J.-K. Park and J. W. Choi, *J. Solid State Electr.*, 2013, **17**, 767-774.

S12 M. A. Hoque, F. M. Hassan, M.-H. Seo, J.-Y. Choi, M. Pritzker, S. Knights, S. Ye and Z. Chen, *Nano Energy*, 2016, **19**, 27-38.

S13 Z. Chen, M Waje, W. Li and Y. Yan, *Angew. Chem. Int. Ed.* 2007, **46**, 4060-4063.

S14 A. Kongkanand, S. Kuwabata, G. Girishkumar and P. Kamat, *Langmuir,* 2006, **22**, 2392-2396.